Appl Phys B (2011) 104:659–663
DOI 10.1007/s00340-011-4457-8

Applied Physics B
Lasers and Optics

Electrically switchable two-dimensional photonic crystals made of polymer-dispersed liquid crystals based on the Talbot self-imaging effect

Y.J. Liu · H.T. Dai · E.S.P. Leong · J.H. Teng · X.W. Sun

Received: 29 October 2010 / Revised version: 10 January 2011 / Published online: 3 June 2011

Abstract Electrically switchable two-dimensional photonic crystals were demonstrated using polymer-dispersed liquid crystal materials based on the Talbot self-imaging effect of a single photomask. With the photomask subjected to a collimated Ar^+ laser beam operating at 488 nm, a three-dimensional spatial light intensity pattern was created due to the Talbot self-imaging effect. The spatial light intensity pattern was then recorded inside a cell filled with the liquid crystal/prepolymer mixture to create photonic crystal structures. The surface morphology of the photonic crystals was examined by an atomic force microscopy. It showed square structures with a lattice constant of ∼0.9 μm. The diffraction and electro-optical properties were also presented. This approach shows a simple and fast fabrication.

1 Introduction

Photonic crystal (PhC), enabling the localization of light [1, 2], has been attracting intensive attention due to the existence of photonic bandgaps (PBGs). Various approaches have been used to fabricate PhCs, such as electron-beam lithography [3, 4], self-organization of colloids [5], layer-by-layer micromachining [6], and holographic lithography [7–10]. Among these methods, laser holography technique offers a highly versatile and flexible approach to create PhC structures. Using this technique, large-area defect-free structures can be produced through a single-step exposure. However, the use of the multiple independent laser beams for the interference pattern generation can introduce optical alignment complexities and inaccuracies as a result of alignment errors in angles among interfering beams as well as vibrational instabilities in the setup. To improve alignment accuracy and stability of the holographic setup, only a single optical element used to produce the multiple-beam interference pattern has been reported, such as diffraction masks [11–15] and specially designed prisms [16–19].

On the other hand, due to their excellent electro-optical properties, polymer-dispersed liquid crystals (PDLCs) [20] have found many applications including smart windows [21], displays [22], microlenses [23–25], random lasers [26–28], and storages [29]. PDLC films can be prepared using methods such as encapsulation, thermally induced phase separation, solvent-induced phase separation, and photopolymerization-induced phase separation (PIPS) [30]. Based on laser interference holography, various periodical structures, such as gratings [31–33], hexagonal [13, 19], transverse square [34, 35], orthorhombic [36, 37], and diamondlike lattices [38], can also be introduced inside the PDLC film through the PIPS method, coined as holographic PDLCs (HPDLCs) [39]. These HPDLC-based PhC structures have been found many applications including switchable lasing emission [40–44] and chemical/humidity sensing [45, 46].

Recently, Yuan and co-workers have reported a 3D PDLC PhC based on the Talbot self-imaging effect [47]. However, since the Talbot distance was ∼8 μm in their work, it is very

Y.J. Liu (✉) H.T. Dai X.W. Sun
School of Electrical & Electronic Engineering,
Nanyang Technological University, Nanyang Avenue,
Singapore 639798, Singapore
e-mail: yjliu@pmail.ntu.edu.sg
Fax: +65-68727528

X.W. Sun (✉)
e-mail: exwsun@ntu.edu.sg
Fax: +65-67933318

Y.J. Liu · E.S.P. Leong · J.H. Teng
Institute of Materials Research and Engineering,
Agency for Science Technology and Research (A*STAR),
3 Research Link, Singapore 117602, Singapore

challenging to fabricate 3D structures in practice because the strong absorption of the photoinitiator caused the uneven distribution in exposure intensity along the film thickness direction. Although it would be possible to further decrease the Talbot distance by decreasing the period of the mask, the optical contrast will decrease greatly as a tradeoff due to the strong diffraction induced by the small period. A compromise limited by the tradeoff is to fabricate 2D instead of 3D structures. In this paper, we demonstrate 2D PhC structures in PDLCs based on the Talbot self-imaging effect of a single mask. The electro-optical properties of such a 2D PhC are further investigated. Application of an electric field can reorientate the LC molecules inside the PDLC PhC, thus modulating the refractive index difference between the polymer matrix and the LC. A total refractive index match between the two materials can be achieved by tuning the LCs to a specific orientation. In such a way, we can switch the 2D PDLC PhC from diffraction to transmission. This approach is an alternative to provide simple and fast fabrication as well as high throughput.

2 Experiments

Figure 1(a) shows the schematic of our experimental setup. The photomask used in our experiment was a chessboard-like binary amplitude-type grating with a period of 1.4 μm and a duty cycle of 50%, as shown in Fig. 1(b). The working area was 4×4 mm^2. Figure 1(c) is the far-field diffraction pattern by performing the Fourier transform of Fig. 1(b). Electron-beam lithography was employed to fabricate the chessboard-like grating. In the electron-beam lithography, an accelerating voltage of 20 KeV and beam current of 200 pA were employed, respectively. Methyl methacrylate resist was spin-coated on a pretreated glass slide to achieve a resist layer of ∼470 nm in thickness. Before exposure, the spun resist on substrate was pre-baked at 150°C for 90 s. The sample was then developed for 150 s and rinsed for 60 s after exposure. Subsequently a metal layer of Ti/Au (30 nm/80 nm) was deposited. Finally the resist was removed from the surface through a lift-off process in acetone.

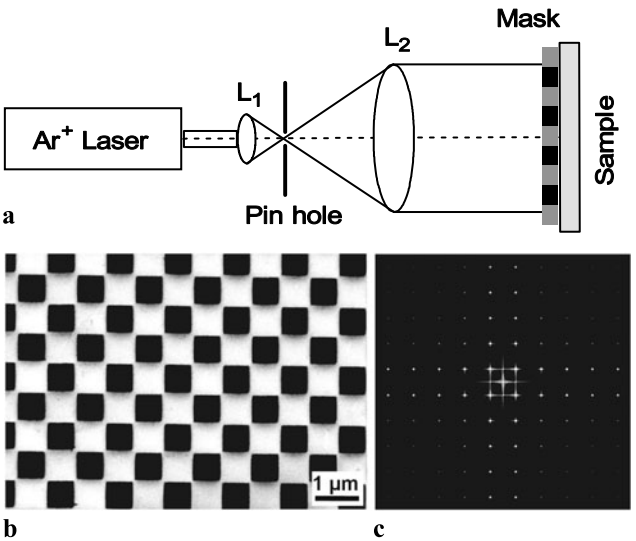

Fig. 1 (**a**) Schematic of the experimental setup, (**b**) a SEM image of the chessboard-like binary amplitude-type grating, and (**c**) far-field diffraction pattern of (**b**)

The starting LC/prepolymer mixture syrup used consisted of 35 wt% monomer, trimethylolpropane triacrylate (TMPTA), 5 wt% cross-linking monomer, N-vinylpyrrollidone (NVP), 0.8 wt% photoinitiator, rose bengal (RB), 1.2 wt% coinitiator, N-phenylglycine (NPG), 8 wt% surfactant, octanoic acid (OA), all from Sigma-Aldrich, and 50 wt% liquid crystal, E7, from Merck. The E7 liquid crystal used has an ordinary refractive index of $n_o = 1.521$, and a birefringence of $\Delta n = 0.225$. All the materials were mechanically blended according to the appropriate weight ratio at 65°C (higher than the clearing point of the liquid crystal E7) to form a homogeneous mixture in dark condition. To record the light intensity pattern in the Talbot distances, thin glass slides with the thickness of 200 μm were used. To investigate the electro-optical properties, an indium-tin-oxide (ITO) layer of ∼80 nm was coated on the slide. Then we sandwiched a drop of the prepolymer/LC mixture between two pieces of ITO glasses. The gap was controlled to be ∼3 μm with glass microsphere spacers. A collimated Ar^+ laser beam (488 nm) was used to illuminate the photomask to produce the diffraction pattern. A cell filled with the LC/prepolymer mixture was placed immediately behind the photomask and subject to the exposure.

To check the surface profiles of the polymeric pattern, we peeled off one piece of ITO glass and sunk the sample into methanol for at least 12 hrs to remove the LCs. After drying, the samples were investigated under an atomic force microscopy (AFM) and scanning electron microscopy (SEM). Electro-optical properties were investigated for the 2D PDLC PhCs.

3 Simulation

When a periodic structure, such as a grating, is illuminated with spatially and temporally coherent light, constructive interference results in intensity patterns that mimic the original period at certain distances beyond the grating, known as the Talbot self-imaging effect [48]. The minimum distance between replications of the fundamental spatial frequency is the Talbot distance

$$Z_T = 2d^2/\lambda, \tag{1}$$

where d is the period of the input pattern and λ is the illuminating wavelength. For instance, Fig. 2(a) shows one-dimensional simulation of the Talbot effect using beam

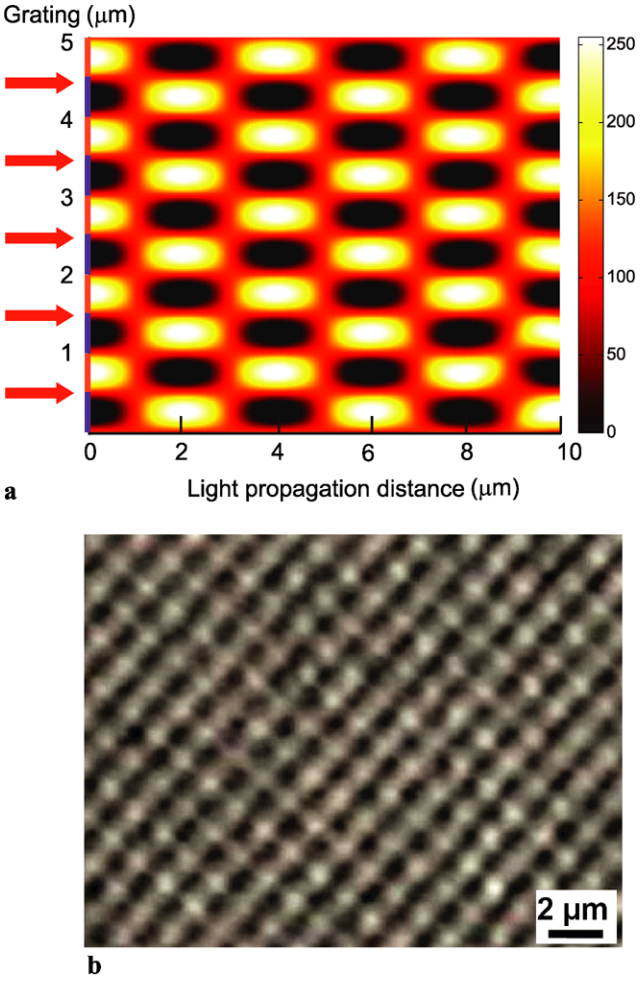

Fig. 2 (**a**) One-dimensional simulation of the Talbot effect of a grating, and (**b**) a typical micrograph of Talbot images for our chessboard-like mask observed under an optical microscope at a certain axial plane

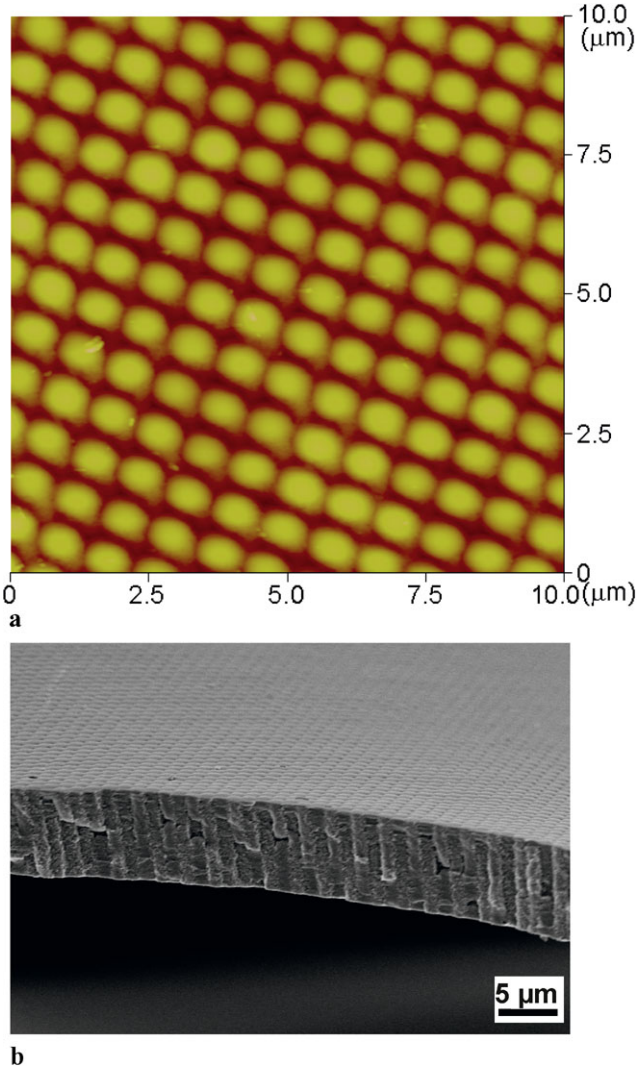

Fig. 3 (**a**) AFM and (**b**) SEM images showing the surface and cross-section morphologies of the PDLC PhC, respectively

propagation method with a grating of period $d = 1.0$ μm and $\lambda = 0.5$ μm. The Talbot distance is $Z_T = 4.0$ μm. After a propagation shift of $Z_T/2$, an image of the grating will be reconstructed but with a lateral shift of half period. Even multiples of $Z_T/2$ reproduce the original spatial frequency fundamental, while odd multiples reproduce the fundamental with a π-phase shift. Figure 2(b) shows a typical micrograph of Talbot images for our chessboard-like mask, which was observed under an optical microscope at a certain axial plane.

3.1 Results and discussion

Figure 3(a) shows the surface morphologies of the 2D PDLC PhCs with the LCs removed. A clear square structure can be observed from Fig. 3(a), which is similar to the photomask structure. The period of the square structure is ∼0.9 μm, which is less than that of the photomask. One reason is that the polymeric pattern shrinks during the photopolymerization process. The other possible reason is that the laser beam was not ideally collimated. In a Gaussian system with the convergent wave, the period of the mth-order imaged pattern can be decreased by a factor of $[1+2d^2m/(\lambda f)]$ [49], where f is the focal length. In addition, the Talbot length in our experiments is ∼8 μm. By choosing suitable cell thickness less than $Z_T/2$, only a single pattern layer can be recorded inside the PDLC cell, and the periodicity along the propagation direction is hence broken down. In our experiment, the cell thickness was ∼3 μm. Therefore, the formed PhC structure was considered to be a 2D pattern. To confirm our claim, we fabricated another sample with the same fabrication conditions and parameters only except that the thickness of the film is ∼8 μm. The selection of such thickness was only for convenient peeling off of the PDLC film from the substrate. Figure 3(b) shows the cross-section SEM image of the sam-

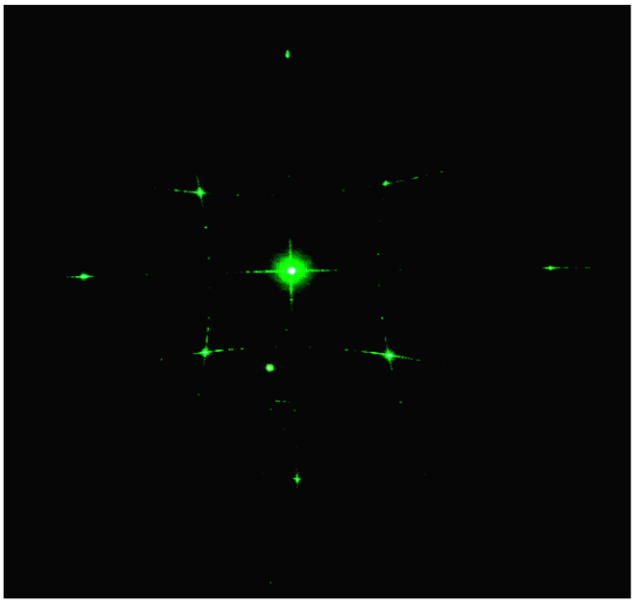

Fig. 4 Diffraction pattern of the PDLC PhC

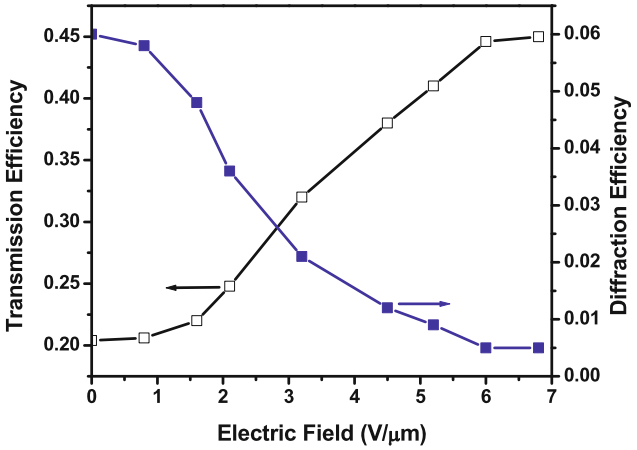

Fig. 5 Diffraction and transmission intensity changes as the function of applied voltages

ple. A columnar structure is clearly observed, confirming a 2D structure even the thickness is much larger than 3 μm.

Figure 4 shows the diffraction patter of the 2D PDLC PhCs produced by a normally incident He-Ne laser operating at 543 nm. We can also see a clear square diffraction pattern, which matches well with the far-field diffraction pattern of the mask (Fig. 1(c)). It is worth mentioning that the arc-shaped light diffraction pattern observed in the far field could be mainly attributed to the non-uniform light intensity distribution induced by the z-direction periodicity. Another possible reason could be the deformation of the self-imaged pattern due to the diffraction effect of the mask after a long self-imaging distance because a glass substrate with the thickness of about 200 μm was inserted between the mask and the recording film in our experiments, which is comparable to 25 Talbot lengths.

The electro-optical effect was also investigated. Figure 5 shows the diffraction and transmission intensity changes as the function of applied voltages. It shows a very similar trend as the H-PDLC samples we observed before [19]. We can see that with the increase of the electric field, the diffraction intensity decreases and the transmission intensity increases accordingly due to the refractive index difference change between the polymer regions and the LC regions. Due to large LC droplets formed during the photopolymerization process, a relatively low threshold (0.8 V/μm) and switching electric field (6.0 V/μm) were achieved, respectively. The low switching field was also attributed to the addition of the surfactant since the surfactant could form an intermediate layer as a lubricant between the LC droplet and polymer network [50, 51]. However, the response time is slower correspondingly compared to most H-PDLC PhCs. The response time measured is about 10 ms by summing the rising time and the falling time. In addition, it is noted from Fig. 5 that the total first-order diffraction efficiency for the 2D PhC is ∼24%. This 2D PDLC PhC can be simply considered as two orthogonally superimposed gratings. For a grating, the magnitude of the diffraction efficiency strongly depends on the diffraction regime determined by the parameter $Q = 2\pi\lambda L/n_o\Lambda^2$, where λ is the wavelength of 0.543 μm, Λ is the grating spacing of ∼0.9 μm, L is the film thickness of ∼3 μm, and n_o is the average refractive index. Here, n_o is estimated to be ∼1.558 from the mixture ratio of LC and polymer molecules. The parameter Q is calculated to be ∼8. As a result, the formed grating is estimated to operate in the intermediate regime between Raman–Nath and Bragg regimes. It is therefore expected that the diffraction efficiency shows a relatively low value when the grating operates in the intermediate regime compared to those in the Bragg regime.

4 Conclusion

Electrically switchable 2D PDLC PhCs have been produced based on the Talbot self-imaging effect of a photomask. This proposed method is suitable for high-efficiency and large-area fabrication. With direct contact or in close proximity immediately behind the mask, much more accurate structures can be achieved using this method. In addition, if a Gaussian optical system were adopted [49], this method would provide additional freedom to easily engineer the patterned structures with adjustable periods based on a single mask. Although such 2D PDLC PhC structures cannot show complete bandgaps due to the low refractive index contrast, they still have potential applications in particle trapping and sorting with high power efficiency. In addition, the all-organic nature of such PhC structures makes them useful

as a sacrificial template to create patterns with high index materials.

References

1. E. Yablonovitch, Phys. Rev. Lett. **58**, 2059 (1987)
2. S. John, Phys. Rev. Lett. **58**, 2486 (1987)
3. S.Y. Lin, J.G. Fleming, D.L. Hetherington, B.K. Smith, R. Biswas, K.M. Ho, M.M. Sigalas, W. Zubrzycki, S.R. Kurtz, J. Bur, Nature **394**, 251 (1998)
4. M. Qi, E. Lidorikis, P.T. Rakich, S.G. Johnson, J.D. Joannopoulos, E.P. Ippen, H.I. Smith, Nature **429**, 538 (2004)
5. A.Y. Vlasov, X.-Z. Bo, J.C. Sturm, D.J. Norris, Nature **414**, 289 (2001)
6. E. Özbay, E. Michel, G. Tuttle, Appl. Phys. Lett. **64**, 2059 (1994)
7. M. Campbell, D.N. Sharp, M.T. Harrison, R.G. Denning, A.J. Turberfield, Nature **404**, 53 (2000)
8. V.Y. Miklyaev, C.D. Meisel, A. Blanco, Appl. Phys. Lett. **82**, 1284 (2003)
9. D.N. Sharp, M. Campbell, R.E. Dedman, Opt. Quantum Electron. **34**, 3 (2002)
10. L.Z. Cai, X.L. Yang, Y.R. Wang, J. Opt. Soc. Am. A **19**, 2238 (2002)
11. V. Berger, O. Gauthier-Lafaye, E. Costard, Electron. Lett. **33**, 425 (1997)
12. I. Divliansky, T.S. Mayer, K.S. Holliday, V.H. Crespi, Appl. Phys. Lett. **82**, 1667 (2003)
13. Y.J. Liu, X.W. Sun, Appl. Phys. Lett. **89**, 171101 (2006)
14. T.Y.M. Chan, O. Toader, S. John, Phys. Rev. E **73**, 046610 (2006)
15. G.Y. Zhou, F.S. Chau, Appl. Phys. Lett. **90**, 181106 (2007)
16. L.J. Wu, Y.C. Zhong, C.T. Chan, K.S. Wong, G.P. Wang, Appl. Phys. Lett. **86**, 241102 (2006)
17. Y. Yang, S.H. Zhang, G.P. Wang, Appl. Phys. Lett. **88**, 251104 (2006)
18. X.H. Sun, X.M. Tao, T.J. Ye, P. Xue, Y.-S. Szeto, Appl. Phys. B **87**, 65 (2007)
19. Y.J. Liu, X.W. Sun, Jpn. J. Appl. Phys. **46**, 6634 (2007)
20. J.W. Doane, N.A. Vaz, B.-G. Wu, S. Zumer, Appl. Phys. Lett. **48**, 269 (1986)
21. D. Cupelli, F.P. Nicoletta, S. Manfredi, M. Vivacqua, P. Formoso, G. De Filpo, G. Chidichimo, Sol. Energy Mater. Sol. Cells **93**, 2008 (2009)
22. C.D. Sheraw, L. Zhou, J.R. Huang, D.J. Gundlach, T.N. Jackson, M.G. Kane, I.G. Hill, M.S. Hammond, J. Campi, B.K. Greening, J. Francl, J. West, Appl. Phys. Lett. **80**, 1088 (2002)
23. H. Ren, Y.-H. Fan, Y.-H. Lin, S.-T. Wu, Opt. Commun. **247**, 101 (2005)
24. G.-R. Xiong, G.-Z. Han, C. Sun, H. Xu, H.-M. Wei, Z.-Z. Gu, Adv. Funct. Mater. **19**, 1082 (2009)
25. Y.J. Liu, T.J. Huang, H.T. Dai, X.W. Sun, Opt. Express **17**, 12418 (2009)
26. D.S. Wiersma, S. Cavalieri, Nature **414**, 708 (2001)
27. S. Gottardo, S. Cavalieri, O. Yaroshchuk, D.S. Wiersma, Phys. Rev. Lett. **93**, 263901 (2004)
28. Y.J. Liu, X.W. Sun, H.I. Elim, W. Ji, Appl. Phys. Lett. **89**, 011111 (2006)
29. Y.J. Liu, X.W. Sun, Appl. Phys. Lett. **90**, 191118 (2007)
30. P.S. Drzaic, *Liquid Crystal Dispersions* (World Scientific, Singapore, 1995)
31. R.L. Sutherland, L.V. Natarajan, V.P. Tondiglia, T.J. Bunning, Chem. Mater. **5**, 1533 (1993)
32. Y.J. Liu, B. Zhang, Y. Jia, K.S. Xu, Opt. Commun. **218**, 27 (2003)
33. Y.J. Liu, X.W. Sun, J.H. Liu, H.T. Dai, K.S. Xu, Appl. Phys. Lett. **86**, 041115 (2005)
34. M.J. Escuti, J. Qi, G.P. Crawford, Appl. Phys. Lett. **83**, 1331 (2003)
35. M.-S. Li, S.-Y. Huang, S.-T. Wu, H.-C. Lin, A.Y.-G. Fuh, Appl. Phys. B **101**, 245 (2010)
36. R.L. Sutherland, V.P. Tondiglia, L.V. Natarajan, S. Chandra, Opt. Express **10**, 1074 (2002)
37. V.P. Tondiglia, L.V. Natarajan, R.L. Sutherland, D. Tomlin, T.J. Bunning, Adv. Mater. **14**, 187 (2002)
38. M.J. Escuti, G.P. Crawford, Mol. Cryst. Liq. Cryst. **421**, 23 (2004)
39. T.J. Bunning, L.V. Natarajan, V.P. Tondiglia, R.L. Sutherland, Annu. Rev. Mater. Sci. **30**, 83 (2000)
40. D.E. Lucchetta, L. Criante, O. Francescangeli, F. Simoni, Appl. Phys. Lett. **84**, 837 (2000)
41. R. Jakubiak, V.P. Tondiglia, L.V. Natarajan, R.L. Sutherland, P. Lloyd, T.J. Bunning, R.A. Vaia, Adv. Mater. **17**, 2807 (2005)
42. S.-T. Wu, A.Y.-G. Fuh, Jpn. J. Appl. Phys. **44**, 977 (2005)
43. Y.J. Liu, X.W. Sun, P. Shum, H.P. Li, J. Mi, W. Ji, X.H. Zhang, Appl. Phys. Lett. **88**, 061107 (2006)
44. Y.J. Liu, X.W. Sun, H.I. Elim, W. Ji, Appl. Phys. Lett. **90**, 011109 (2007)
45. V.K.S. Hsiao, W.D. Kirkey, F. Chen, A.N. Cartwright, P.N. Prasad, T.J. Bunning, Adv. Mater. **17**, 2211 (2005)
46. J. Shi, V.K.S. Hsiao, T.J. Huang, Nanotechnology **18**, 465501 (2007)
47. X.C. Yuan, D.G. Zhang, Y.Y. Sun, J. Bu, S.W. Zhu, J. Opt. A, Pure Appl. Opt. **11**, 105104 (2009)
48. W.H.F. Talbot, Philos. Mag. **9**, 401 (1836)
49. V.P. Kandidov, A.V. Kondrat'ev, Quantum Electron. **31**, 1032 (2001)
50. J. Klosterman, L.V. Natarajan, V.P. Tondiglia, R.L. Sutherland, T.J. White, C.A. Guymon, T.J. Bunning, Polymer **45**, 7213 (2004)
51. Y.J. Liu, X.W. Sun, H.T. Dai, J.H. Liu, K.S. Xu, Opt. Mater. **27**, 1451 (2005)